Development 140, 3903-3914 (2013) doi:10.1242/dev.095026

TGFβ signaling is required for sprouting lymphangiogenesis during lymphatic network development in the skin

Jennifer M. James, Ani Nalbandian and Yoh-suke Mukouyama*

SUMMARY

Dermal lymphatic endothelial cells (LECs) emerge from the dorsolateral region of the cardinal veins within the anterior trunk to form an intricate, branched network of lymphatic vessels during embryogenesis. Multiple growth factors and receptors are required for specification and maintenance of LECs, but the mechanisms coordinating LEC movements and morphogenesis to develop three-dimensional lymphatic network architecture are not well understood. Here, we demonstrate in mice that precise LEC sprouting is a key process leading to stereotypical lymphatic network coverage throughout the developing skin, and that transforming growth factor β (TGFβ) signaling is required for LEC sprouting and proper lymphatic network patterning *in vivo*. We utilized a series of conditional mutants to ablate the TGFβ receptors *Tgfbr1* (*Alk5*) and *Tgfbr2* in LECs. To analyze lymphatic defects, we developed a novel, whole-mount embryonic skin imaging technique to visualize sprouting lymphangiogenesis and patterning at the lymphatic network level. Loss of TGFβ signaling in LECs leads to a severe reduction in local lymphangiogenic sprouting, resulting in a significant decrease in global lymphatic network branching complexity within the skin. Our results also demonstrate that TGFβ signaling negatively regulates LEC proliferation during lymphatic network formation. These data suggest a dual role for TGFβ signaling during lymphatic network morphogenesis in the skin, such that it enhances LEC sprouting and branching complexity while attenuating LEC proliferation.

KEY WORDS: TGFβ, Dermal lymphangiogenesis, LEC sprouting

INTRODUCTION

Lymphatic vessels originate from embryonic veins and form an intricate, branched network throughout the body (Srinivasan et al., 2007). Lymphatic vessels are required for lipid absorption as well as immune cell trafficking and surveillance. Lymphatics maintain tissue fluid homeostasis by returning extravasated blood components (or lymph) back into blood circulation via the thoracic duct, preventing edema both in embryos and in the adult (Cueni and Detmar, 2006; Tammela et al., 2007). Pathological lymphangiogenesis occurs during chronic inflammation and tumor metastasis (Oliver and Alitalo, 2005; Das and Skobe, 2008; Alitalo and Detmar, 2012), with some tumors able to modulate lymphangiogenesis by secreting appropriate factors (Mandriota et al., 2001; Skobe et al., 2001; He et al., 2005; Burton et al., 2008). Consequently, the role of lymphatics in both homeostasis and disease necessitates identification of novel molecular pathways controlling lymphangiogenesis.

Lymphatic development initiates when a subset of venous endothelial cells expresses the transcription factor PROX1, a master regulator of lymphatic endothelial cell (LEC) fate (Wigle and Oliver, 1999). PROX1^{+} LECs form pre-lymphatic clusters that balloon from the cardinal veins, and also migrate from veins as small groups of LECs, to form primary lymph sacs (François et al., 2012; Yang et al., 2012). LECs then sprout and migrate to invade the skin and most internal organs within the embryo, covering tissues with a branched network of lymphatic vessels (Sabin, 1902; Mäkinen et al., 2007; Oliver and Srinivasan, 2008). Intriguingly, little is known about cellular mechanisms and molecular pathways that control dynamic lymphatic network formation, where the peripheral lymphatic vasculature is thought to be generated by lymphatic vessel sprouting and migration from primary lymph sacs. In-depth study of this patterning process requires a lymphatic vasculature model that provides a directly observable lymphatic network with an anatomically recognizable pattern.

The vascular endothelial growth factor C (VEGFC) and VEGF receptor 3 (VEGFR3; also known as Flt4) pathway is a major regulator of lymphatic development (Dumont et al., 1998; Mäkinen et al., 2001; Karkkainen et al., 2004). In *Vegfc* homozygous mutants, PROX1^{+} LECs are initially specified within the veins but then fail to form primary lymph sacs, resulting in a lack of lymphatic network development (Karkkainen et al., 2004). VEGFC/VEGFR3 signaling is at least partly responsible for fine-tuning lymphatic network branching through interactions with the VEGFC co-receptor neuropilin 2 (NRP2) (Xu et al., 2010). In *Nrp2* homozygous mutants, lymphatic capillaries are dilated, hyperproliferative and fail to branch properly (Yuan et al., 2002). Given that complex morphogenetic processes are required to form the lymphatic network, other factors either promoting or inhibiting lymphatic vessel sprouting are likely to be involved.

TGFβ signaling is active in LECs (Oka et al., 2008; Niessen et al., 2010) and also plays pivotal roles in cardiovascular development (Lebrin et al., 2005; Pardali et al., 2010). However, the role of TGFβ signaling during lymphatic network development *in vivo* is unclear. TGFβ induces the formation of a heteromeric complex containing type 1 and type 2 serine/threonine-kinase transmembrane receptors (Heldin et al., 1997; Shi and Massagué, 2003; Feng and Derynck, 2005; Ikushima and Miyazono, 2010). Upon TGFβ ligand binding to TGFβR2 (a type 2 receptor) with high affinity, TGFβR2 transphosphorylates a type 1 receptor, leading to its activation. Subsequently, the type 1 receptor propagates the signal into the cell

Laboratory of Stem Cell and Neuro-Vascular Biology, Genetics and Developmental Biology Center, National Heart, Lung and Blood Institute, National Institutes of Health, Building 10/6C103, 10 Center Drive, Bethesda, MD 20892, USA.

*Author for correspondence (mukoyamay@mail.nih.gov)

Accepted 8 July 2013

by phosphorylating receptor-regulated Smads (R-Smads), which then form heteromeric complexes with the common mediator SMAD4 (Co-Smad). In endothelial cells, TGFβ signals through two distinct type 1 receptors: either via the conventional TGFβR1 [which is also known as activin receptor-like kinase 5 (ALK5)], activating SMAD2 and SMAD3, or via ALK1 [which is also known as activin A receptor, type II-like 1 (ACVRL1)] through activation of SMAD1 and SMAD5. Previous studies in culture and *in vivo* tumor lymphangiogenesis models demonstrate that TGFβ signaling negatively regulates lymphangiogenesis (Oka et al., 2008), whereas postnatal lymphatic development requires *Alk1*-mediated TGFβ signaling for maintenance of LEC identity (Niessen et al., 2010). These studies, however, did not address whether TGFβ signaling is required for lymphatic vessel patterning and network morphogenesis during development. Genetic studies in mice demonstrate that loss of essential TGFβ receptors, such as *Tgfbr2* (Oshima et al., 1996), *Tgfbr1* (Larsson et al., 2001) or *Alk1* (Oh et al., 2000; Urness et al., 2000), result in embryonic lethality due to defective heart morphogenesis and severe vascular abnormalities. These early-onset phenotypes in cardiovascular development make it difficult to study whether TGFβ signaling directly contributes to lymphatic vessel development *in vivo*.

To circumvent early embryonic lethality in conventional mutants, we used conditional and inducible *Cre* lines crossed with floxed alleles *Tgfbr2* and *Tgfbr1* to disrupt TGFβ signaling in LECs as they first emerge from the veins and commence network formation. To assess lymphatic network patterning defects, we developed a novel embryonic imaging technique for analysis of lymphatic network development within mouse skin. Utilizing these genetic and technical approaches, we found that perturbations in TGFβ signaling during lymphangiogenesis led to a significant reduction in local LEC sprouting and, in turn, a significant reduction in lymphatic network branching complexity. We also found that TGFβ signaling negatively regulates LEC proliferation during lymphangiogenesis in the skin. This study provides strong evidence that TGFβ signaling is required for lymphatic sprouting and enhances proper lymphatic network morphogenesis within the skin while concurrently restricting LEC proliferation.

MATERIALS AND METHODS

Experimental animals

Characterizations of *Tgfbr1* floxed mice (Larsson et al., 2003), *Tgfbr2* floxed mice (Levéen et al., 2002), *VECadCreERT2*^{tg} mice (Monvoisin et al., 2006), *Prox1*$^{+/GFPCre}$ mice (Srinivasan et al., 2010), *Prox1-CreER*^{T2} mice (Srinivasan et al., 2007), *Tgfb1* mutant mice (Kulkarni et al., 1993), *Tgfb2* mutant mice (Sanford et al., 1997), *Tgfb3* mutant mice (Proetzel et al., 1995) and *Rosa-lacZ R26R* mice (Soriano, 1999) have been reported elsewhere. To induce Cre-mediated excision, we administered 200 μl tamoxifen solution (10 mg/ml for *VECadCreERT2*^{tg} or 15 mg/ml for *Prox1-CreER*^{T2}) by intraperitoneal injection into pregnant dams at embryonic stage (E) 12.5. Embryos were harvested at E14.5. All animals and procedures for mouse experiments were approved by the National Heart, Lung, and Blood Institute (NHLBI) Animal Care and Use Committee.

Immunofluorescence and confocal imaging

Whole-mount embryonic dorsal skin

E13.5-15.5 mouse embryos were fixed in 4% paraformaldehyde in PBS at 4°C overnight. Dorsal skin tissue was dissected from the green shaded region in Fig. 1A (schematic). Extra layers of muscle and tissue were carefully removed with forceps, leaving the superficial lymphatic network layer within the dorsal skin intact. Samples were blocked in 10% heat-inactivated donkey serum or goat serum in PBS containing 0.2% Triton X-100 for 2 hours at room temperature. Samples were then incubated in blocking buffer containing primary antibodies (supplementary material Table S1) overnight at 4°C. For immunofluorescence detection, Alexa-488-, Alexa-568- or Dylight 649-conjugated secondary antibodies (Invitrogen, 1:250; or Jackson ImmunoResearch, 1:300; 1 hour at room temperature) were used. Whole-mount samples were mounted on glass slides with ProLong Gold (Invitrogen) for imaging. All confocal microscopy was carried out on a Leica TCS SP5 confocal (Leica).

Mouse tissue sections

Section staining was described previously (Mukouyama et al., 2005). In brief, E12.5 embryos were fixed with 4% paraformaldehyde in PBS at 4°C overnight, equilibrated in 30% sucrose in PBS and then embedded in OCT compound. Embryos were cryosectioned at 14-16 μm. See supplementary material Table S1 for primary antibodies used on sections. Secondary antibody labeling and confocal imaging was performed as described above.

Lymphatic network analysis and statistics

For LEC counting or lymphatic sprouting analysis, PROX1^{+} cells were counted along the distal migration front (supplementary material Fig. S3A, yellow shaded region). PROX1^{+} cells emerging from the parent vessel or at the vessel tip that co-labeled with LYVE1 were counted as tip cells to obtain the percentage tip cells of total LECs. For lymphatic network branch point analysis, lymphatic vessels were measured in ImageJ to obtain total vessel length. The number of lymphatic branch points was counted to obtain the value branch points per unit length (supplementary material Fig. S3B). All statistical analyses were carried out as Student's *t*-tests, where $*P \leq 0.05$, $**P \leq 0.01$ and $***P \leq 0.001$. Error bars represent s.e.m.

Cell culture

Human, dermal, micro-vascular LECs (mVECs-hDLy cells, Lonza) were cultured in basal media (EGM-2 supplemented with an EGM-2MV BulletKit, Lonza). For RNA extraction and qPCR, cells were incubated for 18 hours in control media, or media supplemented with either 0.1 ng/ml or 1.0 ng/ml recombinant human TGFβ2 (Peprotech). RNA extraction and qPCR were carried out as described below. For ^{3}H-thymidine incorporation assay, cells were cultured for 24 hours in control media, or media supplemented with 1.0 ng/ml recombinant human TGFβ1, TGFβ2 or TGFβ3 (Peprotech). ^{3}H-thymidine was added to cells during the last 4 hours of incubation. Cells were washed and lysed overnight in 0.3 M NaOH. ^{3}H-thymidine was measured using a scintillation-beta counter.

Fluorescence-activated cell sorting (FACS)

Dorsal skin was dissected from E14.5 mouse embryos. Skin cells were dissociated in a dispase/collagenase solution for 45 minutes at 37°C. Macrophages and blood cells were depleted from the dissociated skin cells using anti-rat IgG magnetic beads (Dynal Biotech) that bound to rat anti-CD11b (eBioSciences, 1:50) and rat anti-Ter119 (eBioSciences, 1:50), respectively. For FACS isolation of LECs, cells were first labeled with a rabbit-anti-LYVE1 antibody (ReliaTech, 1:200), and then with goat anti-rabbit IgG-Alexa488 (Invitrogen, 1:250). Cells were then labeled with PE rat anti-mouse CD31 (BD Biosciences, 1:50) and sorted through a MoFlo FACS machine (Beckman Coulter) directly into Trizol.

RT-PCR and qPCR

RNA was extracted from LECs in Trizol. CDNA was generated using SuperScript III First-Strand Synthesis SuperMix (Invitrogen). qPCR was performed on a 7500 Real Time PCR Machine (Applied Biosciences) using SYBR Green reagents (Roche). Primers used for RT-PCR and qPCR in primary, FACS-isolated mouse cells or human dermal LECs (mVEC-hDLy cells) are listed in supplementary material Table S2.

RESULTS

Embryonic skin as a model for lymphatic network dynamics

To visualize the dermal lymphatic vessel network, we developed a whole-mount dissection and antibody labeling protocol for use with the anterior dorsal skin of mouse embryos (Fig. 1A, green highlighted region in schematic). LECs begin to invade the anterior dorsal skin by embryonic day (E) 12.5, forming a stereotypical

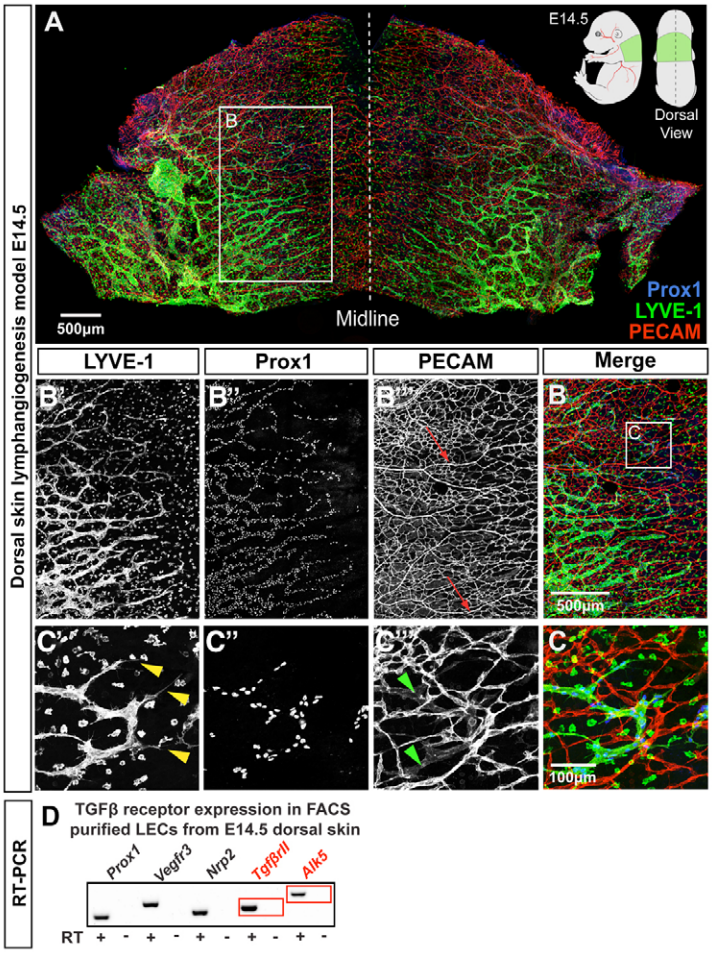

Fig. 1. Embryonic dorsal skin lymphangiogenesis model. (**A**) Confocal tiled *z*-stack image (20×) of a whole-mount anterior dorsal skin (green region in schematic diagram, upper right corner) dissected from an E14.5 mouse embryo and immunolabeled with anti-PROX1 (blue), anti-LYVE1 (green) and anti-PECAM1 (red) antibodies. Dashed line represents the dorsal midline. (**B**) Confocal tiled *z*-stack image (20×) of the lymphatic migration front (boxed area in A). Lymphatic vessels are actively forming a network and are migrating towards, but have not reached, the dorsal midline at E14.5. (**B′-B‴**) Individual channels representing LYVE1, PROX1 and PECAM1, respectively. Red arrows in B‴ indicate remodeled blood vessels. (**C**) Confocal *z*-stack image (40×) of lymphatic sprouts (i.e. 'tip cells') along the lymphatic migration front. (**C′**) Yellow arrowheads label individual LYVE1$^+$ lymphatic tip cells. (**C″**) PROX1$^+$ lymphatic nuclei. Note: Individual LYVE1$^+$ cells are tissue macrophages and are negative for PROX1 (compare C′ and C″). (**C‴**) PECAM1$^+$ lymphatic vessels, green arrowheads. (**D**) RT-PCR analysis of PECAM1$^+$/LYVE1$^+$ LECs FACS-isolated from E14.5 dorsal skin. Primary LECs express *Tgfbr2* and *Tgfbr1* mRNA (red boxes) in addition to the LEC-specific genes *Prox1*, *Vegfr3* and *Nrp2*.

network of PROX1$^+$/LYVE1$^+$ lymphatic vessels that reach the dorsal midline by E15.5-E16.0 (supplementary material Fig. S1). By E14.5, the lymphatic network covers the majority of the dorsal skin, yet migratory LECs have not yet reached the dorsal midline (Fig. 1A; supplementary material Fig. S1B). The dermal lymphatics along the migratory front (Fig. 1B) are actively moving towards the dorsal midline via LEC migration and sprouting lymphangiogenesis, reflecting a dynamic stage in lymphatic network patterning.

We also found that lymphatic network migration follows blood vessel remodeling within the skin, where lymphatic vessels are present only in regions where the primitive blood capillary plexus has remodeled into large-diameter vessels (Fig. 1B,B‴; supplementary material Fig. S1A-C′; red arrows indicate remodeled blood vessels). At E14.5, lymphatic vessels contain many sprouts, or lymphatic 'tip cells' (Fig. 1C,C′, yellow arrowheads) as blood vessels have endothelial tip cells in angiogenic regions (Gerhardt et al., 2003). Single, LYVE1$^+$ macrophages are also prevalent in the skin during lymphatic network development; however, unlike LECs, macrophages do not express the transcription factor PROX1 (compare Fig. 1C′ with 1C″). Lymphatic vessels express the pan-endothelial surface marker PECAM1 (CD31) at this stage (Fig. 1C‴, green arrowheads). We found that there are some clusters of PROX1$^+$ LECs, which appear to be separate from LEC sprouts around the lymphatic vascular front (Fig. 1B″,C″). These clusters may arise from local blood vasculature within the skin or migrate laterally from intersomitic vessels (Yang et al., 2012). Utilizing the dermal lymphatic network as a model system, we can investigate how molecular pathways such as TGFβ signaling regulate developmental lymphangiogenesis.

LECs in the skin express major TGFβ receptors

To determine whether TGFβ receptors are expressed in skin LECs during developmental lymphangiogenesis, we isolated primary embryonic LECs from dorsal skins of E14.5 embryos by two-color fluorescence-activated cell sorting (FACS). We used antibodies against LYVE1 and PECAM1 (CD31) to isolate LYVE1$^+$/PECAM1$^+$ LECs. We determined, by reverse transcriptase PCR (RT-PCR), that FACS-isolated LECs express *Tgfbr2* and *Tgfbr1* (*Alk5*) mRNA (Fig. 1D, red boxes). The FACS-isolated LECs also express *Prox1*, *Vegfr3* and *Nrp2* mRNA, confirming that we were indeed isolating LECs from the dorsal skin (Fig. 1D).

LEC-specific depletion of major TGFβ receptors disrupts lymphatic network development

To understand the role of TGFβ signaling during developmental lymphangiogenesis, we conditionally ablated *Tgfbr2* or *Tgfbr1* in PROX1$^+$ LECs by utilizing a *Prox1*$^{+/GFPCre}$ deleter strain (Srinivasan et al., 2010) in which one copy of *Prox1* is replaced with a *GFPCre* reporter cassette. *Prox1* haploinsufficiency leads to edema and moderate lymphatic defects (Srinivasan et al., 2010), so we were careful to use both *Prox1*$^{+/+}$ (wild-type) and *Prox1*$^{+/GFPCre}$ (haploinsufficient) embryos as controls (compare Fig. 2A,B,D; compare 2F,G,I). The *Prox1*$^{+/GFPCre}$ animals were crossed with

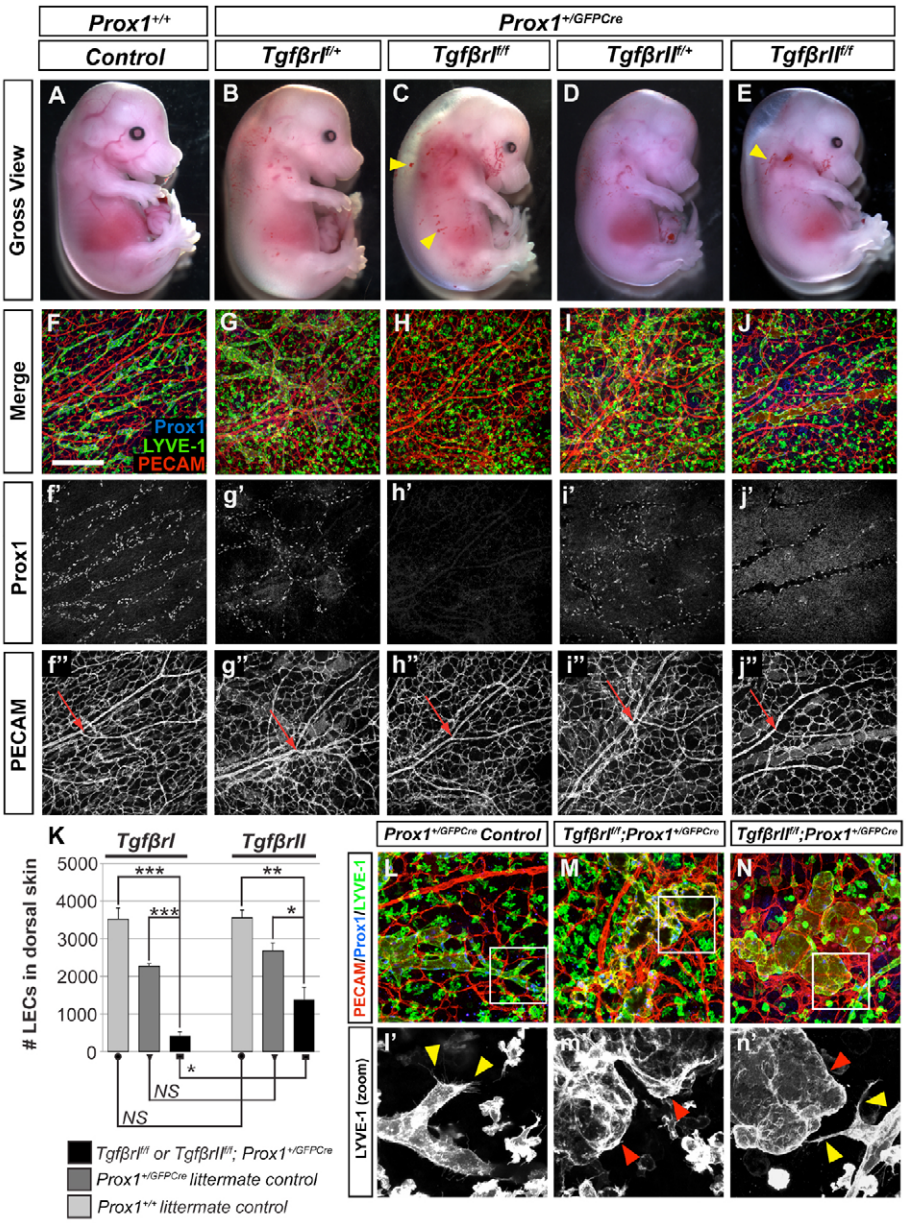

Fig. 2. LEC-specific deletion of major TGFβ receptors prevents lymphatic network development in the skin. (**A-E**) Gross analysis of E14.5 *Prox1*$^{+/GFPCre}$; *Tgfbr1*$^{f/f}$ or *Tgfbr2*$^{f/f}$ mutants (C,E) compared with littermate controls (A,B,D). Discontinuous, blood-filled lymphatics in mutant skin are labeled with yellow arrowheads (C,E). (**F-J**) Confocal *z*-stack images (20×) of whole-mount E14.5 anterior dorsal skins in mutants (H,J) compared with littermate controls (F,G,I) immunolabeled with anti-PROX1 (blue), anti-LYVE1 (green), and anti-PECAM1 (red) antibodies. Dorsal midline is oriented to the right. (**F′-J′**) Fewer PROX1^{+} nuclei are present in *Prox1*$^{+/GFPCre}$; *Tgfbr2*$^{f/f}$ or *Tgfbr1*$^{f/f}$ mutant skins (H′,J′) compared with littermate controls (F′,G′,I′). (**F″-J″**) PECAM1^{+} blood vessels in mutant (H″,J″) and control (F″,G″,I″) embryos. Red arrows indicate remodeled blood vessels. (**K**) Quantification of LEC number in the dorsal skin (n=3). Student's *t*-test, error bars represent s.e.m. *P≤0.05, **P≤0.01, ***P≤0.001. *NS*, not significant. (**L-N**) Confocal *z*-stack (40×) analysis of lymphatic sprouting/tip cell morphology in *Prox1*$^{+/GFPCre}$; *Tgfbr1*$^{f/f}$ or *Tgfbr2*$^{f/f}$ mutants (M,N) compared with *Prox1*$^{+/GFPCre}$ littermate controls (L). Whole-mount dorsal skins were immunolabeled with anti-PROX1 (blue), anti-LYVE1 (green) and anti-PECAM1 (red) antibodies. (**L′-N′**) Insets show 40× *z*-stack confocal images with a 2× optical zoom of LYVE1^{+} lymphatic sprouts. Yellow arrowheads label morphologically normal lymphatic sprouts (L′,N′) and red arrowheads indicate disorganized, blunt lymphatics that do not form interconnections with surrounding LECs (M′,N′). Scale bar: 250 μm.

Tgfbr2 or *Tgfbr1* floxed mice (Levéen et al., 2002; Larsson et al., 2003) to obtain *Prox1*$^{+/GFPCre}$; *Tgfbr2*$^{f/+}$ or *Prox1*$^{+/GFPCre}$; *Tgfbr1*$^{f/+}$ double heterozygous animals. We then generated *Prox1*$^{+/GFPCre}$; *Tgfbr2*$^{f/f}$ and *Prox1*$^{+/GFPCre}$; *Tgfbr1*$^{f/f}$ embryos as LEC-specific TGFβ receptor mutants. This genetic manipulation results in the conditional deletion of either major TGFβ receptor early in lymphatic development (~E9.5-E10.5) as PROX1 is first expressed in endothelial cells. At this early time point, LECs are beginning to emerge from cardinal veins and form primary lymph sacs. We confirmed Cre activity in *Prox1*$^{+/GFPCre}$ dermal LECs using the *Rosa-lacZ R26R-lacZ* reporter line (Soriano, 1999) (supplementary material Fig. S2A-H).

Dissection of embryos at E14.5 revealed moderate edema in the *Prox1*$^{+/GFPCre}$ and *Prox1*$^{+/GFPCre}$; *Tgfbr2*$^{f/+}$ or *Tgfbr1*$^{f/+}$ control embryos (Fig. 2B,D) and severe edema in the *Prox1*$^{+/GFPCre}$; *Tgfbr2*$^{f/f}$ or *Tgfbr1*$^{f/f}$ mutants (Fig. 2C,E). Furthermore, we found blood in lymphatic vessels in a subset of *Prox1*$^{+/GFPCre}$ and *Prox1*$^{+/GFPCre}$; *Tgfbr2*$^{f/+}$ or *Tgfbr1*$^{f/+}$ embryos (Fig. 2B,D). These findings are consistent with reports that *Prox1* haploinsufficiency results in moderate lymphatic defects, including edema and poor separation between blood vessels and lymphatics (Srinivasan et al., 2010). However, abnormalities in the lymphatic vasculature were more severe in *Prox1*$^{+/GFPCre}$; *Tgfbr2*$^{f/f}$ or *Tgfbr1*$^{f/f}$ mutants. Numerous, disconnected, blood-filled lymphatic clusters were present in the skin (Fig. 2C,E, yellow arrowheads).

PROX1, LYVE1 and PECAM1 immunolabeling of dorsal skin at E14.5 revealed that LECs failed to form a branched lymphatic network in *Prox1*$^{+/GFPCre}$; *Tgfbr2*$^{f/f}$ or *Tgfbr1*$^{f/f}$ mutant skin (Fig. 2H,J), whereas *Prox1*$^{+/GFPCre}$; *Tgfbr2*$^{f/+}$ or *Tgfbr1*$^{f/+}$ embryos developed a lymphatic plexus similar to *Prox1*$^{+/GFPCre}$ littermate controls (Fig. 2G,I; data not shown). It appeared that fewer LECs were present within the lymphatic network in *Prox1*$^{+/GFPCre}$; *Tgfbr2*$^{f/f}$ or *Tgfbr1*$^{f/f}$ mutants compared with littermate controls (Fig. 2F′-J′). In fact, many regions of the *Prox1*$^{+/GFPCre}$; *Tgfbr1*$^{f/f}$ mutant skin were completely devoid of LECs (Fig. 2H′). We quantified the number of PROX1^{+} nuclei within the distal migration

front (supplementary material Fig. S3A, yellow shaded region) and found a significant reduction in both *Prox1*$^{+/GFPCre}$; *Tgfbr2*$^{f/f}$ and *Prox1*$^{+/GFPCre}$; *Tgfbr1*$^{f/f}$ mutants compared with *Prox1*$^{+/GFPCre}$ and *Prox1*$^{+/+}$ littermate controls (Fig. 2K). We also detected a significant difference between the number of cells present in the *Prox1*$^{+/GFPCre}$; *Tgfbr2*$^{f/f}$ and *Tgfbr1*$^{f/f}$ mutant skin, indicating that the *Prox1*$^{+/GFPCre}$; *Tgfbr1*$^{f/f}$ mutant phenotype was more severe than the *Prox1*$^{+/GFPCre}$; *Tgfbr2*$^{f/f}$ mutant phenotype at E14.5 (Fig. 2K). Although the lymphatic network was severely perturbed, the blood vascular plexus in the dorsal skin appeared normal in the *Prox1*$^{+/GFPCre}$; *Tgfbr2*$^{f/f}$ or *Tgfbr1*$^{f/f}$ homozygous mutants, with stereotypical remodeled vessels and highly branched capillaries (Fig. 2F″-J″, red arrows). These results demonstrate that TGFβ signaling via *Tgfbr2* and *Tgfbr1* is required in LECs to regulate lymphatic network development.

We wanted to understand further how these severe lymphatic phenotypes arose in LEC-specific TGFβ-signaling mutants. To examine this, we analyzed E12.5 mutant embryo sections for LEC specification and primary lymph sac defects. Primary lymph sac development was largely normal in the *Prox1*$^{+/GFPCre}$; *Tgfbr2*$^{f/f}$ or *Tgfbr1*$^{f/f}$ mutants compared with *Prox1*$^{+/GFPCre}$ controls (supplementary material Fig. S4A-D, lymph sacs labeled with white arrows). We counted the number of LECs in mutant lymph sacs just anterior to heart level and found no significant difference between LEC number in mutants and controls at this stage (supplementary material Fig. S4E). Furthermore, we quantified the percentage of apoptotic LECs at E12.5 and found no significant difference between mutants and controls (supplementary material Fig. S4F-H). These results suggested that initial specification of LECs and primary lymph sac formation occurs in TGFβ signaling mutants but that lymphatic network development might become defective after primary lymph sac formation. This might be due, in part, to improper separation of the lymphatics from the blood vasculature, as we found that TER119^{+} red blood cells completely filled mutant lymph sacs (supplementary material Fig. S4I-L, white arrows). However, some *Prox1*$^{+/GFPCre}$ control embryos also contain blood in the lymph sacs and lymphatic vasculature, so it is unlikely that a separation defect is solely responsible for the lack of lymphatic network development in the skin of mutant embryos. Poor separation between the blood and lymphatic vasculature might be indicative of a heart defect. We analyzed E12.5 hearts and found that overall heart size was slightly decreased in *Prox1*$^{+/GFPCre}$ embryos compared with wild-type hearts; however, we could detect no differences between haploinsufficient and mutant hearts. Further section analysis of E12.5 heart ventricle sections revealed that compact and trabeculated myocardium are not defective (supplementary material Fig. S5A-J).

LEC morphology is perturbed when TGFβ receptors are ablated

As we did not detect an early lymphatic defect, we further analyzed the mutant lymphatics at E14.5 to determine whether lymphangiogenic sprouting (i.e. tip cell formation) was affected when the major TGFβ receptors were ablated (Fig. 2L-N). Though the sparse lymphatic vessels that formed in *Prox1*$^{+/GFPCre}$; *Tgfbr2*$^{f/f}$ or *Tgfbr1*$^{f/f}$ mutant dorsal skin did contain a few lymphatic sprouts with characteristic tip cells (Fig. 2N′, yellow arrowheads), the majority of mutant lymphatic vessels had a blunt appearance and a complete absence of filopodia – a hallmark of wild-type lymphatic vessels undergoing sprouting lymphangiogenesis (compare Fig. 2M′,N′ with 2L′, red arrowheads). These results indicated that a TGFβ signaling deficiency prevents lymphatic sprouting and network development within the skin. Mutant LECs might not form proper filopodia or other cellular extensions that could be a requirement for LEC sprouting and organized network development. However, due to the severe lymphatic defects in the *Prox1*$^{+/GFPCre}$; *Tgfbr2*$^{f/f}$ or *Tgfbr1*$^{f/f}$ mutant skin, we were unable to determine definitively whether TGFβ signaling was directly involved in lymphangiogenic sprouting using this genetic cross.

Pan-endothelial depletion of *Tgfbr2* or *Tgfbr1* after primary lymph sac formation leads to reduced lymphatic network branching complexity

To circumvent severe lymphatic network defects caused by early depletion of major TGFβ receptors, we utilized a pan-endothelial, tamoxifen-inducible *CreER* line, *VECadCreERT2*^{tg} (Monvoisin et al., 2006), to drive Cre expression in VE-cadherin (*Cdh5*)-expressing cells, including LECs and blood endothelial cells (BECs), as the lymphatic network was actively developing in the skin. A temporally controlled, Cre-mediated excision event was achieved by administering tamoxifen by intraperitoneal injection at E12.5, as the lymphatic network first invades the dorsal skin. By initiating Cre-mediated excision at E12.5, many LECs and BECs expressing *VECadCreERT2*^{tg} should undergo Cre-mediated excision of the loxP flanked cassette within 12-36 hours after administration of tamoxifen, resulting in deletion of *Tgfbr2* or *Tgfbr1* in lymphatic and blood vasculature in the skin by E14.5. The timing of this deletion allows us to bypass crucial stages (E9.5-E11.5) of heart and blood-vascular development, as well as early stages of lymphatic development, enabling analysis of later-stage lymphatic network development in the skin. Analysis of *Cre* activity, obtained by crossing the *VECadCreERT2*^{tg} line with the *Rosa-lacZ* (*R26R*) reporter line (Soriano, 1999), showed that Cre is active in the majority of LECs and BECs in the dorsal skin at E14.5 when tamoxifen is administered at E12.5 (supplementary material Fig. S2I-L).

We found that *VECadCreERT2*^{tg}; *Tgfbr2*$^{f/f}$ or *Tgfbr1*$^{f/f}$ mutants displayed mild to moderate edema, whereas littermate controls appeared normal (compare Fig. 3E,I with 3A). Skin dissection and whole-mount immunofluorescence labeling for PROX1^{+}/LYVE1^{+}/PECAM1^{+} lymphatic vessels and PROX1^{-}/LYVE1^{-}/PECAM1^{+} blood vessels revealed that specifically the lymphatic vessels, but not the blood vascular network, were perturbed in the mutants compared with littermate controls (compare Fig. 3F-H,J-L with 3B-D). Mutant lymphatic vessels exhibited hyperplasia and appeared to have reduced branching complexity. A lymphatic network branch point analysis (supplementary material Fig. S3B) revealed that overall lymphatic network branching complexity was significantly reduced by 17.6% in *VECadCreERT2*^{tg}; *Tgfbr1*$^{f/f}$ mutants and by 24.5% in the *VECadCreERT2*^{tg}; *Tgfbr2*$^{f/f}$ mutants compared with littermate controls (Fig. 3M). These results strongly suggested that TGFβ signaling is important for regulating lymphatic network branching complexity during lymphangiogenesis in the skin.

Lymphatic tip cell morphology is perturbed in Cre-inducible *Tgfbr2* and *Tgfbr1* mutants

We next wanted to determine whether LEC morphology in the *VECadCreERT2*^{tg}-mediated, pan-endothelial TGFβ receptor deletion was altered as it was in the *Prox1*$^{+/GFPCre}$; *Tgfbr2*$^{f/f}$ or *Tgfbr1*$^{f/f}$ mutants. Though not as severe as the LEC-specific phenotype, we observed morphological differences in LECs comprising both the proximal lymphatic network (Fig. 4A,C,E; supplementary material Fig. S3A, blue shaded region) and distal tip

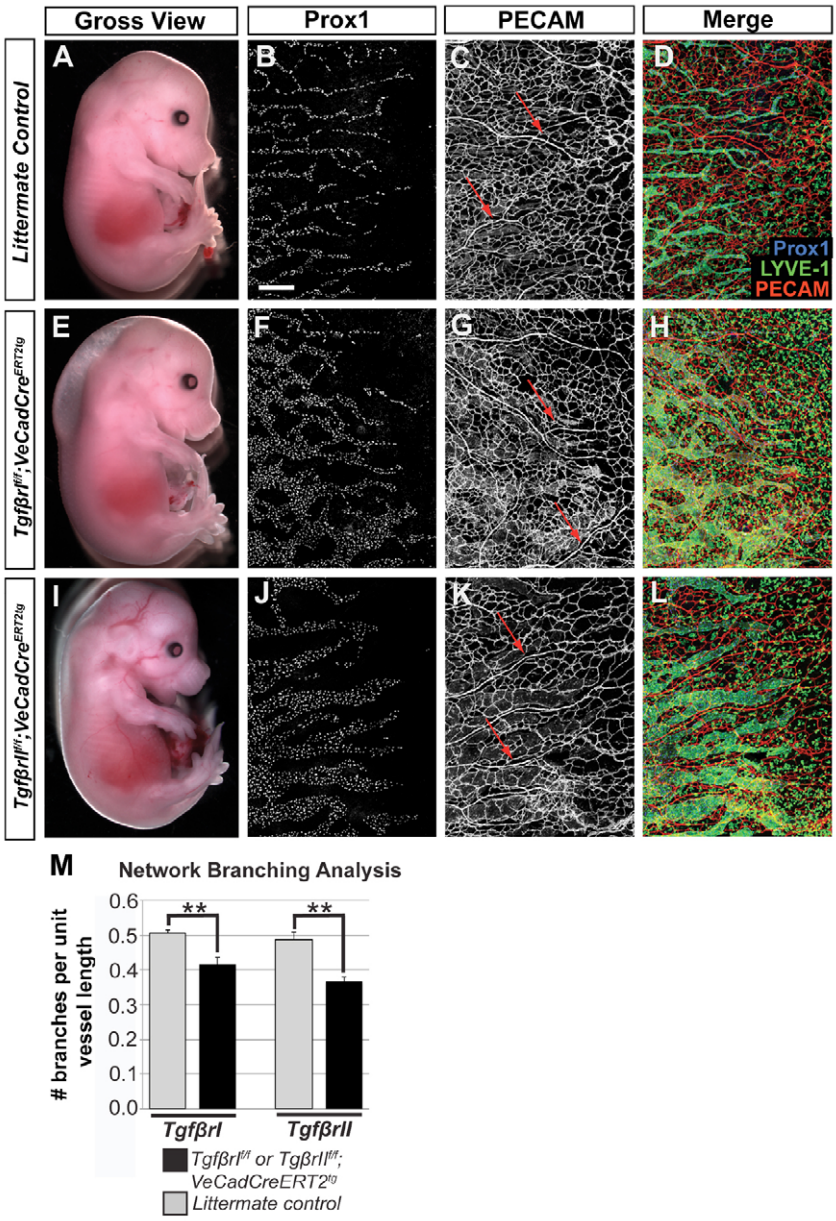

Fig. 3. Cre-inducible depletion of *Tgfbr2* or *Tgfbr1* leads to lymphatic hyperplasia and reduced lymphatic network branching complexity. (**A**,**E**,**I**) Gross analysis of E14.5 *VECadCreERT2^{tg}; Tgfbr2$^{f/f}$* or *Tgfbr1$^{f/f}$* mutants (E,I) compared with littermate control (A). (**D**,**H**,**L**) Confocal tiled *z*-stack images (20×) of whole-mount anterior dorsal skins at E14.5 in mutants (H,L) compared with littermate control (D) labeled with anti-PROX1 (blue), anti-LYVE1 (green) and anti-PECAM1 (red). Mutant skins appear to exhibit lymphatic vessel hyperplasia and reduced network branching complexity (H,L) compared with control (D). (**B**,**F**,**J**) PROX1$^+$ LEC nuclei. (**C**,**G**,**K**) PECAM1$^+$ blood vessels are normal and contain remodeled vessels (red arrows). (**M**) Lymphatic network branching analysis in *VECadCreERT2^{tg}; Tgfbr1* mutant embryos compared with littermate controls (n=4), and *VECadCreERT2^{tg}; Tgfbr2* mutant embryos compared with littermate controls (n=3) shows that lymphatic network branching is significantly reduced in mutants. Student's *t*-test, error bars represent s.e.m. $^{**}P \leq 0.01$. Scale bar: 250 μm.

cells along the migration front (Fig. 4B,D,F; supplementary material Fig. S3A, yellow shaded region). We found that whereas lymphatic vessels actively sprout and anastomose with surrounding vessels within the proximal (closest to limb) lymphatic network in control embryos (Fig. 4A,A′, yellow arrowheads), there were fewer sprouts in the mutants (Fig. 4C,C′,E,E′, yellow arrowhead). In addition, a few blunt-ended, bulbous lymphatic vessels were present in these mutants that were similar to the disorganized, mutant lymphatic vessels found in *Prox1$^{+/GFPCre}$*; *Tgfbr2$^{f/f}$* or *Tgfbr1$^{f/f}$* mutants (Fig. 4C′,E′, red arrows).

There also were fewer lymphatic tip cells along the distal migration front (closest to midline) in mutants compared with littermate controls (Fig. 4B′,D′,F′, yellow arrowheads). We counted PROX1$^+$/LYVE1$^+$ tip cells within the distal migration front (supplementary material Fig. S3A, yellow shaded region). We defined a lymphatic 'tip cell' as a PROX1$^+$ nucleus emerging from the parent vessel or at the leading edge of a migrating lymphatic vessel that also displays prominent LYVE1$^+$ cellular extensions. We then counted total PROX1$^+$ nuclei in this region. We found that the percentage of tip cells out of total LECs was reduced by 41.1% in *VECadCreERT2^{tg}; Tgfbr1* mutants and by 48.2% in *VECadCreERT2^{tg}; Tgfbr2* mutants compared with littermate controls (Fig. 4G). These results suggest that local disruptions in LEC sprouting at the single-cell level might lead to a global reduction in lymphatic network complexity in TGFβ signaling mutants. In addition, these results suggest that TGFβ signaling is required for proper LEC sprouting in embryonic mouse skin.

LEC proliferation is increased in pan-endothelial *Tgfbr2* and *Tgfbr1* mutants

We next investigated the hyperplastic lymphatic vessel phenotype by determining whether LECs were over-proliferating. PROX1$^+$ single-positive (Fig. 4H,J) and PROX1$^+$/Ki67$^+$ double-positive nuclei (Fig. 4I,K, white arrowheads) were counted on one half of the anterior dorsal skin in mutant and control littermates. Though we found that wild-type LEC proliferation in this region is low (~1% of LECs are

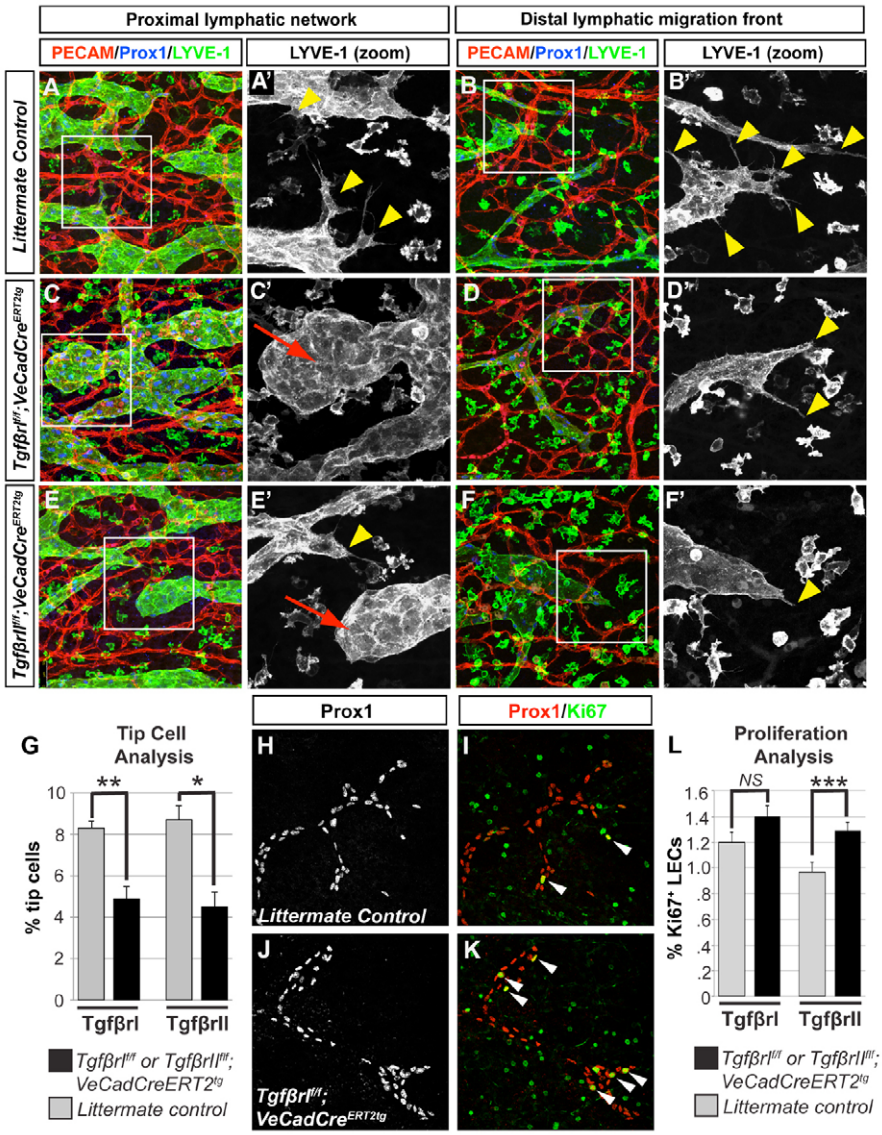

Fig. 4. Cre-inducible depletion of *Tgfbr2* or *Tgfbr1* leads to aberrant lymphatic vessel morphology and hyper-proliferative LECs. (**A-F**) Confocal *z*-stack (40×) analysis of lymphatic sprouting/tip cell morphology in the proximal lymphatic network (vessels closer to the limb and further from the midline; A,C,E) and the distal lymphatic migration front (the region closest to and migrating towards the midline; B,D,F) in *VECadCreERT2^{tg}; Tgfbr2$^{f/f}$* or *Tgfbr1$^{f/f}$* mutants (C-F) compared with littermate controls (A,B). Whole-mount dorsal skins were immunolabeled with anti-PROX1 (blue), anti-LYVE1 (green) and anti-PECAM1 (red) antibodies. (**A′-F′**) Insets show 40× *z*-stack confocal images with a 2× optical zoom of LYVE1$^+$ lymphatic sprouts. Yellow arrowheads label morphologically normal lymphatic sprouts. (A′,C′,E′) Red arrows indicate disorganized, blunt lymphatic vessels that do not form interconnections with surrounding LECs. (B′,D′,F′) Migrating lymphatic vessels contain fewer sprouts in mutants (D′,F′) compared with controls (B′) (yellow arrowheads). (**G**) Percentage lymphatic tip cells out of total PROX1$^+$ LECs in the distal migration front in *VECadCreERT2^{tg}; Tgfbr2$^{f/f}$* (*n*=3) or *Tgfbr1$^{f/f}$* (*n*=4) mutants compared with littermate controls. (**H-K**) Representative 40× confocal *z*-stack images of PROX1$^+$ (H,J) or PROX1$^+$/Ki67$^+$ proliferative LECs (I,K, white arrowheads) in *VECadCreERT2^{tg}; Tgfbr1$^{f/f}$* mutants (J,K) compared with littermate controls (H,I). (**L**) Percentage proliferative LECs in *VECadCreERT2^{tg}; Tgfbr2$^{f/f}$* (*n*=3) or *Tgfbr1$^{f/f}$* (*n*=4) mutants compared with littermate controls. Student's *t*-test, error bars represent s.e.m. **P*≤0.05, ***P*≤0.01, ****P*≤0.001. *NS*, not significant.

proliferative) at E14.5, we were able to quantify an LEC proliferation defect in the TGFβ signaling mutants compared with controls. We found that overall LEC proliferation was significantly increased by 33.5% in *VECadCreERT2^{tg}; Tgfbr2$^{f/f}$* mutants compared with littermate controls. Although *VECadCreERT2^{tg}; Tgfbr1$^{f/f}$* mutants showed a 17% proliferation increase compared with controls, this was not a significant difference (Fig. 4L). These results suggest that a decrease in lymphatic sprouting and branching complexity coupled with a slight increase in LEC proliferation leads to the lymphatic vessel hyperplasia seen in the *VECadCreERT2^{tg}; Tgfbr2$^{f/f}$* or *Tgfbr1$^{f/f}$* mutant skin.

LEC-specific, inducible TGFβ receptor deletion leads to lymphatic network perturbations in dorsal skin

We confirmed the results from the analysis of *VECadCreERT2^{tg}; Tgfbr2$^{f/f}$* or *Tgfbr1$^{f/f}$* mutants by using the *Prox1-CreER^{T2}* deleter strain to specifically ablate TGFβ signaling in LECs beginning at E12.5 as the lymphatic network first invades the dorsal skin. We administered 200 µl of a 15 mg/ml tamoxifen solution into pregnant dams at E12.5, and harvested embryos at E14.5. Upon embryo dissection, we found that *Prox1-CreER^{T2}; Tgfbr2$^{f/f}$* and *Tgfbr1$^{f/f}$* mutants were indistinguishable from littermate controls and displayed no severe edema or visible vascular abnormalities (data not shown). However, upon dissection and immunolabeling of the dorsal skin, we found that lymphatic network development was perturbed in *Prox1-CreER^{T2}; Tgfbr2$^{f/f}$* and *Tgfbr1$^{f/f}$* mutants compared with littermate controls (Fig. 5A-F). We found a significant decrease in lymphatic network complexity in *Prox1-CreER^{T2}; Tgfbr1$^{f/f}$* mutants (Fig. 5G). Consistent with the *Prox1$^{+/GFPCre}$* and *VECadCreERT2^{tg}* data, we also saw defects in lymphatic sprouting (Fig. 5A′-F′). We found that LEC sprouting was significantly decreased in *Prox1-CreER^{T2}; Tgfbr1$^{f/f}$* mutants compared with littermate controls. Though we quantified a comparable decrease in LEC sprouting in *Prox1-CreER^{T2}; Tgfbr2$^{f/f}$* mutants compared with controls, it was not significant. However, we were able to identify isolated regions within *Prox1-CreER^{T2}; Tgfbr2$^{f/f}$* dorsal skin containing dysmorphogenic lymphatic vessels (Fig. 5E′, red arrowhead) and reduced lymphatic branching along the migration front (Fig. 5F′). These data strongly suggest that TGFβ signaling, specifically within LECs, coordinates precise lymphatic network branching in the dorsal skin.

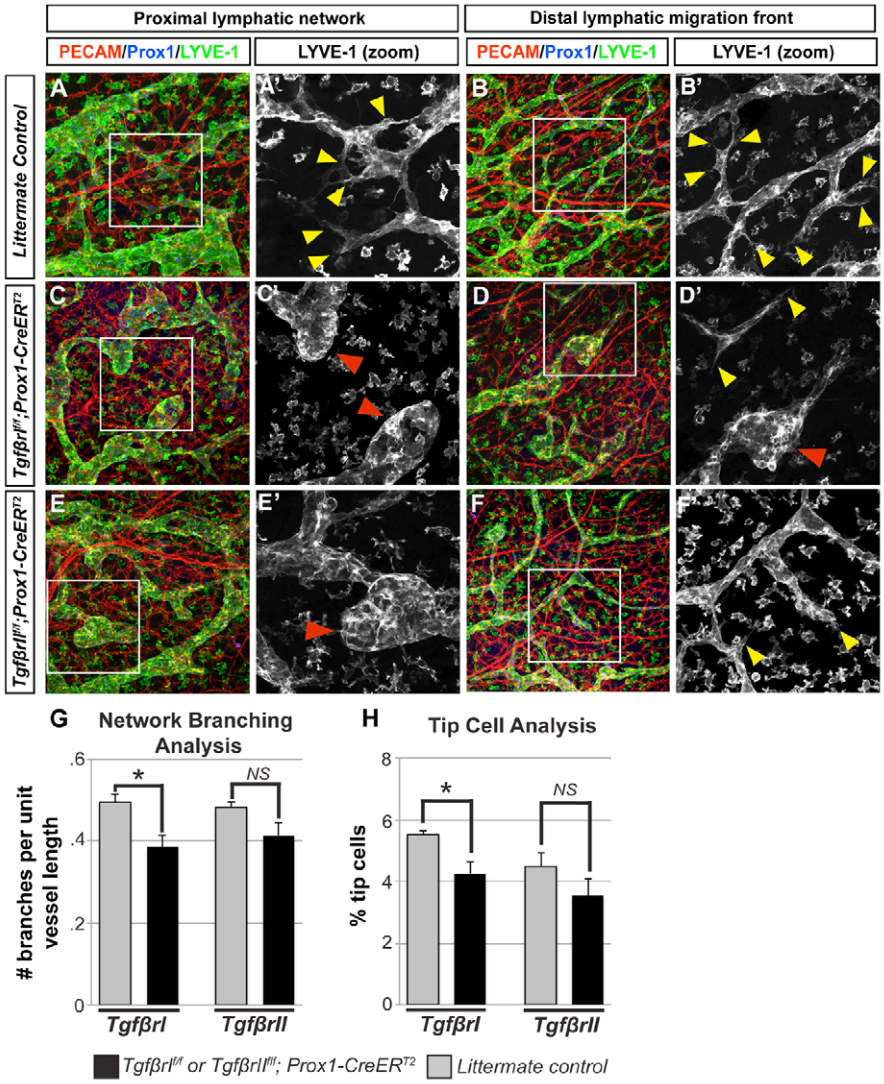

Fig. 5. LEC-specific, inducible TGFβ receptor deletion leads to lymphatic network perturbations. (**A-F**) Confocal *z*-stack (40×) analysis of lymphatic sprouting/tip cell morphology in the lymphatic network at E14.5 in *Prox1-CreER^{T2}; Tgfbr2$^{f/f}$* and *Tgfbr1$^{f/f}$* mutants (C-F) compared with littermate controls (A,B). Whole-mount dorsal skins were immunolabeled with anti-PROX1 (blue), anti-LYVE1 (green) and anti-PECAM-1 (red) antibodies. (**A′-F′**) Insets show 40× *z*-stack confocal images with a 2× optical zoom of LYVE1$^+$ lymphatic sprouts. Yellow arrowheads label morphologically normal lymphatic sprouts. (A′,C′,E′) Red arrowheads indicate disorganized, blunt lymphatic vessels that do not form interconnections with surrounding LECs as seen in the *Prox1$^{+/GFPCre}$* (see Fig. 2) and *VECadCreER^{tg}* (see Fig. 4) crosses. (B′,D′,F′). Migrating lymphatic vessels contain fewer sprouts in mutants (D′,F′) compared with controls (B′) (yellow arrowheads). (**G**) Lymphatic network branching analysis in *Prox1-CreER^{T2};Tgfbr1* mutant embryos compared with littermate controls (*n*=3), and *Prox1-CreER^{T2}; Tgfbr2* mutant embryos compared with littermate controls (*n*=3) shows that lymphatic network branching is significantly reduced in mutants. (**H**) Percentage lymphatic tip cells out of total PROX1$^+$ LECs in the distal migration front in *Prox1-CreER^{T2}; Tgfbr2$^{f/f}$* (*n*=3) or *Tgfbr1$^{f/f}$* (*n*=3) mutants compared with littermate controls. Student's *t*-test, error bars represent s.e.m. *$P \leq 0.05$. *NS*, not significant.

Tgfb2 conventional mutants display defects in lymphatic network development

Mosaic ablation of TGFβ signaling in the dermal lymphatic network, as we analyzed in *VECadCreERT2^{tg}* and *Prox1-CreER^{T2}*; *Tgfbr2$^{f/f}$* or *Tgfbr1$^{f/f}$* mutants, might cause only partial penetrance of lymphatic defects and could explain why lymphatic defects are less severe than within the *Prox1$^{+/GFPCre}$*; *Tgfbr2$^{f/f}$* or *Tgfbr1$^{f/f}$* mutants. To address this issue by an independent approach, we analyzed lymphatic vessel development in conventional mutants for the three major TGFβ ligands: *Tgfb1* (Kulkarni et al., 1993), *Tgfb2* (Sanford et al., 1997) or *Tgfb3* (Proetzel et al., 1995). We found that the *Tgfb2$^{-/-}$*, but not *Tgfb1$^{-/-}$ or Tgfb3$^{-/-}$*, mutant embryos displayed mild edema compared with littermate controls (Fig. 6A,C; data not shown). Immunostaining of the dorsal skin revealed that *Tgfb2$^{-/-}$*, but not *Tgfb1$^{-/-}$* or *Tgfb3$^{-/-}$*, mutant embryos displayed lymphatic network defects (Fig. 6B,D-H). *Tgfb2$^{-/-}$* mutants exhibited reduced branching complexity and enlarged vessels within the lymphatic vasculature, whereas blood vascular remodeling occurred normally (Fig. 6B″,D″, red arrows). Analysis of LEC morphology showed reduced lymphatic sprouts in the mutants (compare Fig. 6J′ and 6I′, yellow arrowheads), with some *Tgfb2$^{-/-}$* lymphatic vessels displaying a blunt-ended morphology (Fig. 6J′, red arrowhead). Network branching and proliferation analysis showed a 16.1% decrease in network branching complexity as well as a 35.8% increase in LEC proliferation in mutants compared with littermate controls, both statistically significant (Fig. 6K,L). Though the lymphatic network was perturbed in the *Tgfb2$^{-/-}$* mutants, the phenotype was not as severe as that of the *Prox1$^{+/GFPCre}$*; *Tgfbr2$^{f/f}$* or *Tgfbr1$^{f/f}$* mutants, indicating that other TGFβ isoforms might play a role in regulating lymphatic network morphogenesis. These data demonstrate that Tgfβ2 plays a significant role in lymphatic development and is required for proper lymphatic network morphogenesis.

TGFβ2 inhibits proliferation and upregulates *VEGFR3* and *NRP2* in human LECs

We next examined whether TGFβ directly influences LEC proliferation. To address this question, we performed a ^{3}H-thymidine DNA synthesis assay as a sensitive and quantitative cell proliferation assay to determine the growth state of a human dermal LEC line in the presence of human TGFβ1, 2 and 3 ligands. This assay showed that all three major TGFβ ligands significantly reduced ^{3}H-thymidine incorporation into human LECs compared with control media. In support of our findings in mouse, TGFβ2 had

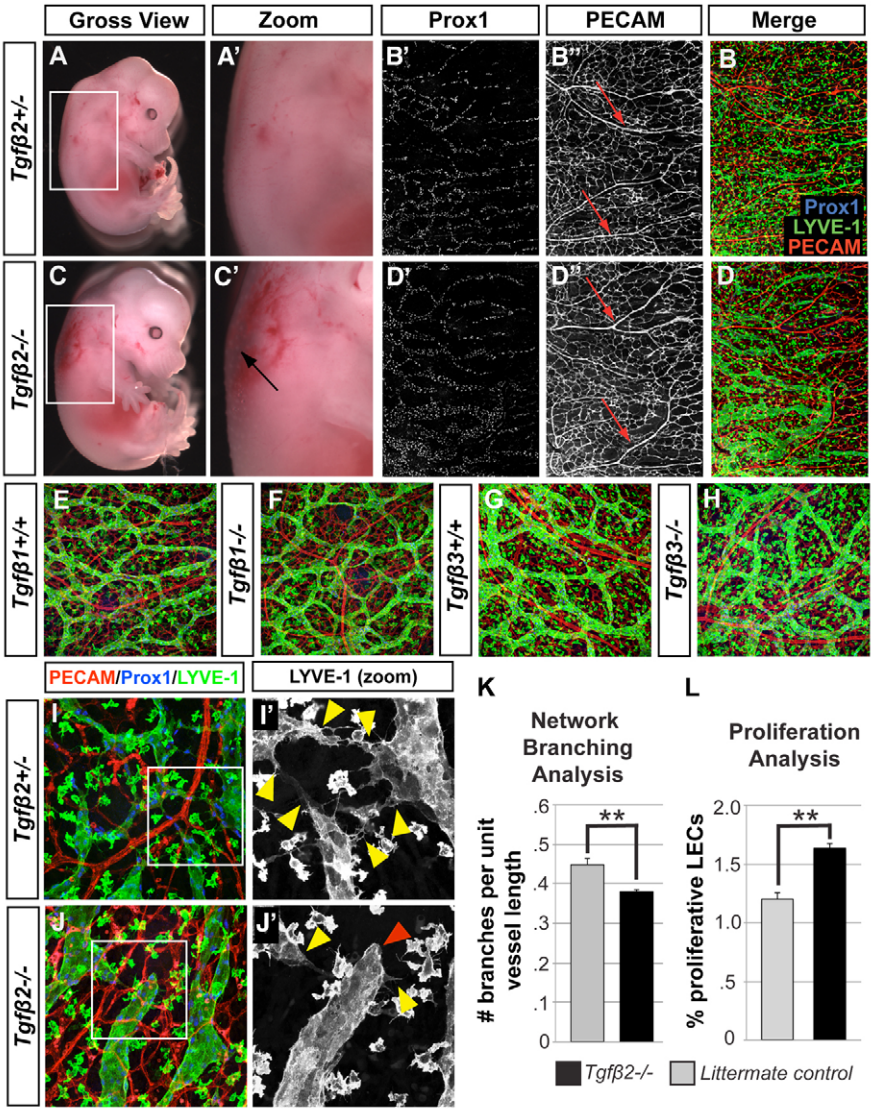

Fig. 6. TGFβ2 is required for proper lymphatic network morphogenesis. (**A**,**C**) Gross analysis of E14.5 *Tgfb2*$^{-/-}$ mutants (E) and littermate controls (A). (**A′**,**C′**) Insets show moderate edema (arrow) in the dorsal region of *Tgfb2*$^{-/-}$ mutants (E′). (**B**,**D**) Confocal tiled *z*-stack images (20×) of whole-mount anterior dorsal skins labeled with anti-PROX1 (blue), anti-LYVE1 (green), and anti-PECAM1 (red) antibodies. Enlarged lymphatic vessels are present in *Tgfb2*$^{-/-}$ mutants (D) compared with littermate controls (B). (**B′**,**D′**) PROX1^{+} LEC nuclei. (**B″**,**D″**) PECAM1^{+} blood vessels are normal in mutant (B″) and control (D″) embryos. Red arrows indicate remodeled blood vessels. (**E-H**) 20× confocal *z*-stack images of *Tgfb1*$^{-/-}$ and *Tgfb3*$^{-/-}$ mutant skin (F,H) compared with littermate controls (E,G). (**I**,**J**) Confocal *z*-stack (40×) analysis of lymphatic sprouting/tip cell morphology in *Tgfb2*$^{-/-}$ mutants (J) compared with controls (I). (**I′**,**J′**) Insets depict 40× *z*-stack confocal images with a 2× optical zoom of LYVE1^{+} lymphatic sprouts. Yellow arrowheads label morphologically normal lymphatic sprouts. Red arrowhead indicates dysmorphogenic lymphatic vessel (J′). Lymphatic vessels contain fewer sprouts in *Tgfb2*$^{-/-}$ mutants (J′) compared with controls (I′). (**K**,**L**) Lymphatic network branching is significantly decreased whereas LEC proliferation is significantly increased in *Tgfb2*$^{-/-}$ mutants compared with controls (n=3). Student's *t*-test, error bars represent s.e.m. **P≤0.01.

the greatest effect on human LEC proliferation, reducing ^{3}H-thymidine incorporation by 46% compared with controls (Fig. 7B).

Because of the importance of the VEGFC/VEGFR3/NRP2 pathway in sprouting lymphangiogenesis (Xu et al., 2010), we next examined whether TGFβ signaling affects the expression of *VEGFR3* (*FLT4*) or *NRP2* in LECs. To test this, we used a human dermal lymphatic cell line expressing TGFβR2 and TGFβR1 (Fig. 7A) to determine whether expression of *VEGFR3* or *NRP2* mRNA changes upon administration of TGFβ2 ligand *in vitro* (Fig. 7C). We observed a significant increase in both *VEGFR3* and *NRP2* mRNA transcript levels compared with untreated controls. How this induction might control lymphatic network complexity *in vivo* is unclear at this time. However, it is possible that local TGFβ stimulates expression of VEGFR3 and NRP2 in dermal LECs, resulting in lymphatic sprouting and appropriate network branching complexity within the skin.

DISCUSSION

The data presented here demonstrate a requirement for TGFβ signaling during lymphatic network development in the skin. Conditional ablation of either major TGFβ receptor during LEC specification dramatically reduces lymphatic network coverage in the skin, even though LEC specification and primary lymph sac formation are normal. However, genetic disruption of *Tgfbr2* or *Tgfbr1* at a later stage, as the lymphatic network is actively developing within the skin, leads to a significant reduction in network branching and tip cell formation. In the *VECadCreERT2*^{tg}; *Tgfbr2*$^{f/f}$ or *Tgfbr1*$^{f/f}$ and *Tgfb2* mutants, TGFβ signaling disruptions can also result in a significant increase in LEC proliferation, resulting in hyperplastic lymphatic vessels. This suggests a dual role for TGFβ signaling during lymphatic network development in the skin, whereby TGFβ signaling enhances LEC sprouting and network complexity while negatively regulating LEC proliferation.

During lymphatic network formation, LEC sprouts or tip cells exhibit dynamic filopodia and migratory behavior but rarely proliferate, similar to blood endothelial tip cells. Our results show that perturbations in TGFβ signaling within LECs leads to a reduction of LEC sprouting and a slight increase in LEC number in the skin, suggesting a dual role for TGFβ signaling that positively induces LEC sprouting or tip cell formation through the upregulation of VEGFR3 and NRP2 while negatively regulating LEC proliferation. Identification of downstream targets to promote

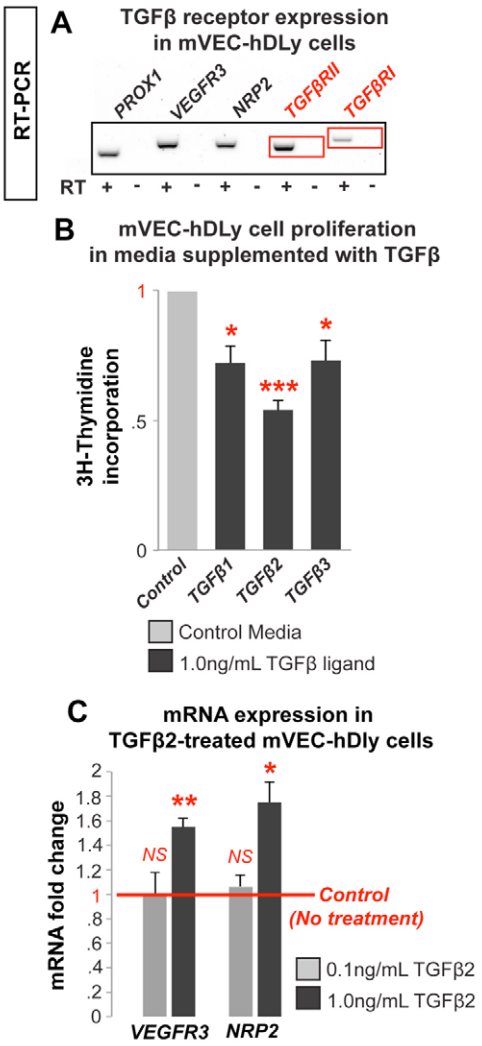

Fig. 7. TGFβ2 inhibits proliferation and upregulates *VEGFR3* and *NRP2* in human dermal LECs. (**A**) RT-PCR analysis of TGFβ receptor expression human dermal LECs (mVEC-hDLYs). *TGFBR2* and *TGFBR1* mRNA are expressed, as well as genes specific for LECs such as *PROX1*, *VEGFR3* and *NRP2*. (**B**) ^{3}H-thymidine incorporation assay using human dermal LECs (mVEC-hDLYs)in the presence of 1.0 ng/ml recombinant human TGFβ1, 2 and 3 ligands. This assay showed that all three major TGFβ ligands significantly reduced ^{3}H-thymidine incorporation into human LECs compared with control media. (**C**) qPCR analysis of *VEGFR3* and *NRP2* mRNA expression in human dermal LECs treated with 1.0 ng/ml recombinant human TGFβ2. *VEGFR3* and *NRP2* expression is significantly increased by 57% and 75%, respectively. Student's *t*-test, error bars represent s.e.m. *P≤0.05, **P≤0.01, ***P≤0.001. *NS*, not significant.

LEC sprouting or to inhibit LEC proliferation will provide insight into the dual role of TGFβ signaling in lymphatic vessel development.

Many cell types present within the skin express TGFβ ligands. Tissue macrophages have been implicated as an important source of pro-angiogenic and pro-lymphangiogenic factors during embryonic and postnatal angiogenesis and lymphangiogenesis (Kubota et al., 2009; Fantin et al., 2010; Gordon et al., 2010). LYVE1^{+} tissue macrophages are closely associated with lymphatic vessels in the developing skin (Fig. 1C) (Gordon et al., 2010). Furthermore, tissue macrophage-deficient mice, such as *Pu.1*$^{-/-}$ and *Csfr1*$^{-/-}$ mutants, exhibit lymphatic network hyperplasia (Gordon et al., 2010). The lymphatic phenotypes in tissue macrophage-deficient mice are similar but less severe than those in *Tgfbr2* and *Tgfbr1* conditional mutants. Tissue macrophages are a source of TGFβs in the skin, given that expression of all major TGFβ ligands are detectable in F480^{+}/LYVE1^{+} tissue macrophages FACS-isolated from embryonic skins (J.M.J. and Y.M., unpublished). We cannot exclude the possibility that other cell types, such as platelets and endothelial cells, are sources of TGFβs during development. A direct demonstration that macrophage-derived TGFβs are required for proper lymphatic vessel formation in the skin will require macrophage-specific knockouts of TGFβs.

TGFβ signaling appears to be involved in many aspects of lymphangiogenesis, including LEC migration and sprouting. Previous work demonstrated that ALK1, another major TGFβ type 1 receptor, which binds to bone morphogenetic protein (BMP) 9 (also known as GDF2), BMP10 and TGFβ, regulates postnatal lymphatic vessel development (Niessen et al., 2010). Inhibition of ALK1 signaling using a soluble decoy ALK1 receptor or ALK1-specific neutralizing antibody results in disruption of lymphatic vessel sprouting in the honeycomb-like network in the tail skins of postnatal pups, whereas this treatment has little effect on the skin blood vasculature. Combined with our observation that *Tgfbr2* and *Tgfbr1* are required for embryonic skin lymphangiogenesis, TGFβ signaling might utilize multiple receptors to regulate lymphatic vessel network formation at different developmental stages. Our work suggests that migratory and sprouting capabilities of LECs are enhanced by TGFβ signaling during lymphatic network formation. As VEGFC has been implicated in lymphatic sprouting by signaling through VEGFR3-NRP2 receptor complexes (Xu et al., 2010), TGFβ signaling might cooperate with VEGFR3/NRP2 signaling to promote lymphatic sprouting. Though we demonstrate that TGFβ2 stimulates *VEGFR3* and *NRP2* expression *in vitro*, further work will be required to understand the molecular mechanism of TGFβ-mediated lymphatic network formation.

During inflammation or tumorigenesis, however, the role of TGFβ signaling in LECs appears to be anti-lymphangiogenic (Clavin et al., 2008; Oka et al., 2008). The somewhat contradictory results reflect the multifaceted role of TGFβ signaling in embryonic and pathological lymphangiogenesis. Lymphangiogenesis induced by VEGFC is potentiated in the presence of the TGFβ receptor 1 kinase inhibitor SB431542 *in vivo* that specifically inhibits *Alk4* (*Acvr1b*), *Alk5* (*Tgfbr1*) and *Alk7* (*Acvr1c*) (Inman et al., 2002; Laping et al., 2002). TGFβ signaling might activate a different combination of Smads and/or cooperate with other intracellular signaling pathways in a context-dependent manner. Therefore, in order to understand the bifunctional roles of TGFβ signaling during embryonic, physiological and pathological lymphangiogenesis, it will be important to identify Smads and their target genes under the activation of TGFβ signaling that might control each individual process.

Acknowledgements

We thank Drs G. Oliver and R. S. Srinivasan for *Prox1*$^{+/GFPCre}$ mice; Drs A. B. Kulkarni and S. Karlsson for *Tgfb1* mutants, *Tgfbr2* floxed and *Tgfbr1* floxed mice; and Dr M. Tanaka for anti-LYVE1 antibody. Thanks to Drs C. Doci and S. Gutkind for helping the ^{3}H-thymidine incorporation assay; L. Samsel, H. Sardon and P. J. McCoy for FACS assistance; J. Hawkins and the staff of NIH Bldg50 animal facility for assistance with mouse breeding and care; K. Gill for laboratory management and technical support; and Y. Carter, L. Oundo and R. Reed for administrative assistance. Thanks also to Drs A. M. Michelson, R. S. Balaban and R. S. Adelstein for invaluable help and discussion; and other members of Laboratory of Stem Cell and Neuro-Vascular Biology for technical help and thoughtful discussion.

Funding
This work was supported by the Intramural Research Program of the National Heart, Lung, and Blood Institute, National Institutes of Health [HL005702-07 to Y.M. Deposited in PMC for release after 12 months.

Competing interests statement
The authors declare no competing financial interests.

Author contributions
J.M.J. performed the majority of experiments for this study and wrote the manuscript. A.N. assisted with some cell culture experiments. Y.M. directed this study and wrote the manuscript.

Supplementary material
Supplementary material available online at
http://dev.biologists.org/lookup/suppl/doi:10.1242/dev.095026/-/DC1

References
Alitalo, A. and Detmar, M. (2012). Interaction of tumor cells and lymphatic vessels in cancer progression. *Oncogene* **31**, 4499-4508.
Burton, J. B., Priceman, S. J., Sung, J. L., Brakenhielm, E., An, D. S., Pytowski, B., Alitalo, K. and Wu, L. (2008). Suppression of prostate cancer nodal and systemic metastasis by blockade of the lymphangiogenic axis. *Cancer Res.* **68**, 7828-7837.
Clavin, N. W., Avraham, T., Fernandez, J., Daluvoy, S. V., Soares, M. A., Chaudhry, A. and Mehrara, B. J. (2008). TGF-beta1 is a negative regulator of lymphatic regeneration during wound repair. *Am. J. Physiol.* **295**, H2113-H2127.
Cueni, L. N. and Detmar, M. (2006). New insights into the molecular control of the lymphatic vascular system and its role in disease. *J. Invest. Dermatol.* **126**, 2167-2177.
Das, S. and Skobe, M. (2008). Lymphatic vessel activation in cancer. *Ann. N. Y. Acad. Sci.* **1131**, 235-241.
Dumont, D. J., Jussila, L., Taipale, J., Lymboussaki, A., Mustonen, T., Pajusola, K., Breitman, M. and Alitalo, K. (1998). Cardiovascular failure in mouse embryos deficient in VEGF receptor-3. *Science* **282**, 946-949.
Fantin, A., Vieira, J. M., Gestri, G., Denti, L., Schwarz, Q., Prykhozhij, S., Peri, F., Wilson, S. W. and Ruhrberg, C. (2010). Tissue macrophages act as cellular chaperones for vascular anastomosis downstream of VEGF-mediated endothelial tip cell induction. *Blood* **116**, 829-840.
Feng, X. H. and Derynck, R. (2005). Specificity and versatility in tgf-beta signaling through Smads. *Annu. Rev. Cell Dev. Biol.* **21**, 659-693.
François, M., Short, K., Secker, G. A., Combes, A., Schwarz, Q., Davidson, T. L., Smyth, I., Hong, Y. K., Harvey, N. L. and Koopman, P. (2012). Segmental territories along the cardinal veins generate lymph sacs via a ballooning mechanism during embryonic lymphangiogenesis in mice. *Dev. Biol.* **364**, 89-98.
Gerhardt, H., Golding, M., Fruttiger, M., Ruhrberg, C., Lundkvist, A., Abramsson, A., Jeltsch, M., Mitchell, C., Alitalo, K., Shima, D. et al. (2003). VEGF guides angiogenic sprouting utilizing endothelial tip cell filopodia. *J. Cell Biol.* **161**, 1163-1177.
Gordon, E. J., Rao, S., Pollard, J. W., Nutt, S. L., Lang, R. A. and Harvey, N. L. (2010). Macrophages define dermal lymphatic vessel calibre during development by regulating lymphatic endothelial cell proliferation. *Development* **137**, 3899-3910.
He, Y., Rajantie, I., Pajusola, K., Jeltsch, M., Holopainen, T., Yla-Herttuala, S., Harding, T., Jooss, K., Takahashi, T. and Alitalo, K. (2005). Vascular endothelial cell growth factor receptor 3-mediated activation of lymphatic endothelium is crucial for tumor cell entry and spread via lymphatic vessels. *Cancer Res.* **65**, 4739-4746.
Heldin, C. H., Miyazono, K. and ten Dijke, P. (1997). TGF-beta signalling from cell membrane to nucleus through SMAD proteins. *Nature* **390**, 465-471.
Ikushima, H. and Miyazono, K. (2010). TGFbeta signalling: a complex web in cancer progression. *Nat. Rev. Cancer* **10**, 415-424.
Inman, G. J., Nicolás, F. J., Callahan, J. F., Harling, J. D., Gaster, L. M., Reith, A. D., Laping, N. J. and Hill, C. S. (2002). SB-431542 is a potent and specific inhibitor of transforming growth factor-beta superfamily type I activin receptor-like kinase (ALK) receptors ALK4, ALK5, and ALK7. *Mol. Pharmacol.* **62**, 65-74.
Karkkainen, M. J., Haiko, P., Sainio, K., Partanen, J., Taipale, J., Petrova, T. V., Jeltsch, M., Jackson, D. G., Talikka, M., Rauvala, H. et al. (2004). Vascular endothelial growth factor C is required for sprouting of the first lymphatic vessels from embryonic veins. *Nat. Immunol.* **5**, 74-80.
Kubota, Y., Takubo, K., Shimizu, T., Ohno, H., Kishi, K., Shibuya, M., Saya, H. and Suda, T. (2009). M-CSF inhibition selectively targets pathological angiogenesis and lymphangiogenesis. *J. Exp. Med.* **206**, 1089-1102.
Kulkarni, A. B., Huh, C. G., Becker, D., Geiser, A., Lyght, M., Flanders, K. C., Roberts, A. B., Sporn, M. B., Ward, J. M. and Karlsson, S. (1993). Transforming growth factor beta 1 null mutation in mice causes excessive inflammatory response and early death. *Proc. Natl. Acad. Sci. USA* **90**, 770-774.
Laping, N. J., Grygielko, E., Mathur, A., Butter, S., Bomberger, J., Tweed, C., Martin, W., Fornwald, J., Lehr, R., Harling, J. et al. (2002). Inhibition of transforming growth factor (TGF)-beta1-induced extracellular matrix with a novel inhibitor of the TGF-beta type I receptor kinase activity: SB-431542. *Mol. Pharmacol.* **62**, 58-64.
Larsson, J., Goumans, M. J., Sjöstrand, L. J., van Rooijen, M. A., Ward, D., Levéen, P., Xu, X., ten Dijke, P., Mummery, C. L. and Karlsson, S. (2001). Abnormal angiogenesis but intact hematopoietic potential in TGF-beta type I receptor-deficient mice. *EMBO J.* **20**, 1663-1673.
Larsson, J., Blank, U., Helgadottir, H., Björnsson, J. M., Ehinger, M., Goumans, M. J., Fan, X., Levéen, P. and Karlsson, S. (2003). TGF-beta signaling-deficient hematopoietic stem cells have normal self-renewal and regenerative ability in vivo despite increased proliferative capacity in vitro. *Blood* **102**, 3129-3135.
Lebrin, F., Deckers, M., Bertolino, P. and Ten Dijke, P. (2005). TGF-beta receptor function in the endothelium. *Cardiovasc. Res.* **65**, 599-608.
Levéen, P., Larsson, J., Ehinger, M., Cilio, C. M., Sundler, M., Sjöstrand, L. J., Holmdahl, R. and Karlsson, S. (2002). Induced disruption of the transforming growth factor beta type II receptor gene in mice causes a lethal inflammatory disorder that is transplantable. *Blood* **100**, 560-568.
Mäkinen, T., Jussila, L., Veikkola, T., Karpanen, T., Kettunen, M. I., Pulkkanen, K. J., Kauppinen, R., Jackson, D. G., Kubo, H., Nishikawa, S. et al. (2001). Inhibition of lymphangiogenesis with resulting lymphedema in transgenic mice expressing soluble VEGF receptor-3. *Nat. Med.* **7**, 199-205.
Mäkinen, T., Norrmén, C. and Petrova, T. V. (2007). Molecular mechanisms of lymphatic vascular development. *Cell. Mol. Life Sci.* **64**, 1915-1929.
Mandriota, S. J., Jussila, L., Jeltsch, M., Compagni, A., Baetens, D., Prevo, R., Banerji, S., Huarte, J., Montesano, R., Jackson, D. G. et al. (2001). Vascular endothelial growth factor-C-mediated lymphangiogenesis promotes tumour metastasis. *EMBO J.* **20**, 672-682.
Monvoisin, A., Alva, J. A., Hofmann, J. J., Zovein, A. C., Lane, T. F. and Iruela-Arispe, M. L. (2006). VE-cadherin-CreERT2 transgenic mouse: a model for inducible recombination in the endothelium. *Dev. Dyn.* **235**, 3413-3422.
Mukouyama, Y. S., Gerber, H. P., Ferrara, N., Gu, C. and Anderson, D. J. (2005). Peripheral nerve-derived VEGF promotes arterial differentiation via neuropilin 1-mediated positive feedback. *Development* **132**, 941-952.
Niessen, K., Zhang, G., Ridgway, J. B., Chen, H. and Yan, M. (2010). ALK1 signaling regulates early postnatal lymphatic vessel development. *Blood* **115**, 1654-1661.
Oh, S. P., Seki, T., Goss, K. A., Imamura, T., Yi, Y., Donahoe, P. K., Li, L., Miyazono, K., ten Dijke, P., Kim, S. et al. (2000). Activin receptor-like kinase 1 modulates transforming growth factor-beta 1 signaling in the regulation of angiogenesis. *Proc. Natl. Acad. Sci. USA* **97**, 2626-2631.
Oka, M., Iwata, C., Suzuki, H. I., Kiyono, K., Morishita, Y., Watabe, T., Komuro, A., Kano, M. R. and Miyazono, K. (2008). Inhibition of endogenous TGF-beta signaling enhances lymphangiogenesis. *Blood* **111**, 4571-4579.
Oliver, G. and Alitalo, K. (2005). The lymphatic vasculature: recent progress and paradigms. *Annu. Rev. Cell Dev. Biol.* **21**, 457-483.
Oliver, G. and Srinivasan, R. S. (2008). Lymphatic vasculature development: current concepts. *Ann. N. Y. Acad. Sci.* **1131**, 75-81.
Oshima, M., Oshima, H. and Taketo, M. M. (1996). TGF-beta receptor type II deficiency results in defects of yolk sac hematopoiesis and vasculogenesis. *Dev. Biol.* **179**, 297-302.
Pardali, E., Goumans, M. J. and ten Dijke, P. (2010). Signaling by members of the TGF-beta family in vascular morphogenesis and disease. *Trends Cell Biol.* **20**, 556-567.
Proetzel, G., Pawlowski, S. A., Wiles, M. V., Yin, M., Boivin, G. P., Howles, P. N., Ding, J., Ferguson, M. W. and Doetschman, T. (1995). Transforming growth factor-beta 3 is required for secondary palate fusion. *Nat. Genet.* **11**, 409-414.
Sabin, F. (1902). On the origin of the lymphatics system from the veins and the development of the lymph hearts and the thoracic duct in the pig. *Am. J. Anat.* **1**, 367-389.
Sanford, L. P., Ormsby, I., Gittenberger-de Groot, A. C., Sariola, H., Friedman, R., Boivin, G. P., Cardell, E. L. and Doetschman, T. (1997). TGFbeta2 knockout mice have multiple developmental defects that are non-overlapping with other TGFbeta knockout phenotypes. *Development* **124**, 2659-2670.
Shi, Y. and Massagué, J. (2003). Mechanisms of TGF-beta signaling from cell membrane to the nucleus. *Cell* **113**, 685-700.
Skobe, M., Hawighorst, T., Jackson, D. G., Prevo, R., Janes, L., Velasco, P., Riccardi, L., Alitalo, K., Claffey, K. and Detmar, M. (2001). Induction of tumor lymphangiogenesis by VEGF-C promotes breast cancer metastasis. *Nat. Med.* **7**, 192-198.
Soriano, P. (1999). Generalized lacZ expression with the ROSA26 Cre reporter strain. *Nat. Genet.* **21**, 70-71.
Srinivasan, R. S., Dillard, M. E., Lagutin, O. V., Lin, F. J., Tsai, S., Tsai, M. J., Samokhvalov, I. M. and Oliver, G. (2007). Lineage tracing demonstrates the

venous origin of the mammalian lymphatic vasculature. *Genes Dev.* **21**, 2422-2432.

Srinivasan, R. S., Geng, X., Yang, Y., Wang, Y., Mukatira, S., Studer, M., Porto, M. P., Lagutin, O. and Oliver, G. (2010). The nuclear hormone receptor Coup-TFII is required for the initiation and early maintenance of Prox1 expression in lymphatic endothelial cells. *Genes Dev.* **24**, 696-707.

Tammela, T., Saaristo, A., Holopainen, T., Lyytikkä, J., Kotronen, A., Pitkonen, M., Abo-Ramadan, U., Ylä-Herttuala, S., Petrova, T. V. and Alitalo, K. (2007). Therapeutic differentiation and maturation of lymphatic vessels after lymph node dissection and transplantation. *Nat. Med.* **13**, 1458-1466.

Urness, L. D., Sorensen, L. K. and Li, D. Y. (2000). Arteriovenous malformations in mice lacking activin receptor-like kinase-1. *Nat. Genet.* **26**, 328-331.

Wigle, J. T. and Oliver, G. (1999). Prox1 function is required for the development of the murine lymphatic system. *Cell* **98**, 769-778.

Xu, Y., Yuan, L., Mak, J., Pardanaud, L., Caunt, M., Kasman, I., Larrivée, B., Del Toro, R., Suchting, S., Medvinsky, A. et al. (2010). Neuropilin-2 mediates VEGF-C-induced lymphatic sprouting together with VEGFR3. *J. Cell Biol.* **188**, 115-130.

Yang, Y., García-Verdugo, J. M., Soriano-Navarro, M., Srinivasan, R. S., Scallan, J. P., Singh, M. K., Epstein, J. A. and Oliver, G. (2012). Lymphatic endothelial progenitors bud from the cardinal vein and intersomitic vessels in mammalian embryos. *Blood* **120**, 2340-2348.

Yuan, L., Moyon, D., Pardanaud, L., Bréant, C., Karkkainen, M. J., Alitalo, K. and Eichmann, A. (2002). Abnormal lymphatic vessel development in neuropilin 2 mutant mice. *Development* **129**, 4797-4806.